# Structural Insights into a Circadian Oscillator

Carl Hirschie Johnson,[1]* Martin Egli,[2] Phoebe L. Stewart[3]

An endogenous circadian system in cyanobacteria exerts pervasive control over cellular processes, including global gene expression. Indeed, the entire chromosome undergoes daily cycles of topological changes and compaction. The biochemical machinery underlying a circadian oscillator can be reconstituted in vitro with just three cyanobacterial proteins, KaiA, KaiB, and KaiC. These proteins interact to promote conformational changes and phosphorylation events that determine the phase of the in vitro oscillation. The high-resolution structures of these proteins suggest a ratcheting mechanism by which the KaiABC oscillator ticks unidirectionally. This posttranslational oscillator may interact with transcriptional and translational feedback loops to generate the emergent circadian behavior in vivo. The conjunction of structural, biophysical, and biochemical approaches to this system reveals molecular mechanisms of biological timekeeping.

Many biological processes undergo daily (circadian) rhythms that are dictated by self-sustained biochemical oscillators. These circadian clock systems generate a precise period of ~24 hours in constant conditions (constant light and temperature) that is nearly invariant at different temperatures (temperature compensation) (1). Circadian clocks also show entrainment to day and night, predominantly mediated by the daily light/dark cycle, so that the endogenous biological clock is phased appropriately to the environmental cycle (2). These properties, especially the period's long time constant and temperature compensation, are difficult to explain biochemically. Full understanding of these unusual oscillators will require knowledge of the structures, functions, and interactions of their molecular components.

## Pervasive Circadian Rhythms in a Bacterium

We study the components of the biological clock in the prokaryotic cyanobacterium *Synechococcus elongatus*, which programs many processes to conform optimally to the daily cycle, including photosynthesis, nitrogen fixation, and gene expression (1–3). Competition assays among different strains of *S. elongatus* rigorously demonstrated that this clock system significantly enhanced the fitness of the cells in rhythmic environments, but not in nonselective constant environments (3). The first circadian rhythm measured in *S. elongatus* was that of *psbAI* promoter activity as assayed by a luciferase reporter in populations of cells (4). More recently, a tour de force imaging study visualized the rhythm of luminescence from single bacterial cells (Fig. 1, A and B) (5).

That study also demonstrated that as single cells divide, the daughter cells maintain the circadian phase of the mother cell (Fig. 1B). Therefore, the circadian clock in cyanobacteria is not perturbed by cell division. That result confirmed studies in populations of cells that showed that the circadian clock ticks away with a period of ~24 hours in cells that are dividing with average doubling times of 6 to 10 hours (6–8). Conversely, the circadian clock gates cell division so that there are some times of the day/night cycle when the cells grow without dividing (6). Therefore, two independent timing circuits coexist in this unicellular bacterium; the circadian pacemaker provides a checkpoint for the cell-division cycle, but there is no feedback of the cell-division timing circuit upon the circadian clock (8).

Although it was the *psbAI* promoter that was initially found to be robustly rhythmic in *S. elongatus* (4), further investigation of transcriptional control discovered that essentially all promoters were modulated by the circadian clock (9). Even a heterologous promoter from *Escherichia coli* is transcribed rhythmically when inserted ectopically into the cyanobacterial chromosome (10). Those observations have now been linked with the discovery that the topology of the entire cyanobacterial chromosome is under the control of this circadian program. The *S. elongatus* chromosome undergoes robust oscillations of compaction and decompaction that can be visualized with DNA-binding dyes (Fig. 1C) (11). Moreover, the superhelical status of DNA experiences correlative circadian oscillations (Fig. 1D) (12). Such large-scale changes in chromosomal structure and torsion are likely to modulate transcriptional rates. It is therefore possible that rhythmic gene-expression patterns are mediated by daily changes in the topology of the chromosome. From this perspective, the cyanobacterial chromosome might be envisioned as an oscillating nucleoid, or "oscilloid," that regulates all promoters—including heterologous

promoters—by torsion-sensitive transcription (12). Gene expression in cyanobacteria is also regulated in a circadian fashion by the putative transcriptional factor RpaA; rhythmic gene expression is attenuated when the *rpaA* gene is deleted (2, 13). The phosphorylation status of RpaA is regulated by the two-component system kinase SasA, whose phosphorylation is controlled in turn by the KaiABC oscillator that is described in the next paragraph (13). These results support an alternative model in which the SasA/RpaA two-component system mediates signals from the KaiABC oscillator to drive genome-wide transcription rhythms. Although the oscilloid and the SasA/RpaA models appear to be mutually exclusive, an analysis of stochastic gene expression in cyanobacteria (14) supports regulation both locally (by DNA topology, for example) and comprehensively (by trans factors such as RpaA).

## Cogs and Gears: The Kai Proteins

The clockwork mechanism that controls these global rhythms of transcription, chromosomal topology, and cell division is composed of three essential proteins—KaiA, KaiB, and KaiC—which were identified in 1998 (15). Their three-dimensional structures, which became available in 2004 (16–21), are the only full-length structures of core circadian clock proteins that have been determined. KaiA is a dimer of intertwined monomers, KaiB has a thioredoxin-like fold and forms dimers and tetramers, and KaiC is a "double-doughnut" hexamer (fig. S1). The structure of KaiC revealed a two-domain fold (N-terminal CI and C-terminal CII lobes) in the monomer and six adenosine 5′-triphosphate (ATP) molecules bound between subunits in both the CI and the CII rings (Fig. 2A). ATP binding within CI serves to stabilize the CI ring that forms the hexamer even in the absence of CII domains (16). When the three Kai proteins are combined together with ATP in a test tube, a molecular oscillator is reconstituted (Fig. 1E) (22). This in vitro oscillator perpetuates a ~24-hour cycle for at least 10 days (23), with KaiC alternating between a hypophosphorylated and a hyperphosphorylated state. KaiC is phosphorylated at serine 431 (S431) and threonine 432 (T432) residues in the CII half (24, 25) (Fig. 3, A and B), whereas the CI ring appears devoid of phosphorylation sites. Phosphorylation of CII residues occurs across the subunit-subunit interface, because S431 and T432 are closest to an ATP molecule that is held by the P loop of the adjacent subunit (Fig. 3A).

KaiC is both an autokinase and an autophosphatase (26–28) that rhythmically hydrolyzes 15 ATP molecules per subunit during a complete in vitro cycle (29). Because only two ATP molecules are needed to phosphorylate S431 and T432, the consumption of the extra ATP molecules may be used to drive conformational changes within KaiC, including monomer exchange (23, 30, 31). KaiA promotes the formation of the KaiC hyper-

[1]Department of Biological Sciences, Box 35-1634, Vanderbilt University, Nashville, TN 37235–1634, USA. [2]Department of Biochemistry, Vanderbilt University, Nashville, TN 37235–0146, USA. [3]Department of Molecular Physiology and Biophysics, Vanderbilt University, Nashville, TN 37235–0615, USA.

*To whom correspondence should be addressed. E-mail: carl.h.johnson@vanderbilt.edu

phosphorylated state, whereas KaiB antagonizes the actions of KaiA and promotes a return to the hypophosphorylated state. Structural and biophysical studies have enhanced our understanding of the KaiA•KaiC complex (Fig. 2) (*32*, *33*) and the KaiB•KaiC complex (Fig. 3, C and D) (*34*), as well as quantified the relative levels of KaiC versus KaiA•KaiC versus KaiB•KaiC versus KaiA•KaiB•KaiC complexes formed during the in vitro reaction cycle (*30*, *31*). In addition, the KaiC phosphorylation cycle comprises four consecutive steps: (i) T432 phosphorylation, (ii) S431 phosphorylation, (iii) T432 dephosphorylation, and (iv) S431 dephosphorylation (*28*, *35*). This information provides the framework for a reanalysis of the Kai protein structures, suggesting how the in vitro clock might work.

## KaiC Interacts with KaiA and KaiB

KaiA binds repeatedly and rapidly to KaiC during the phosphorylation phase (*30*) and enhances KaiC's autokinase activity. Moreover, a single KaiA dimer appears to be sufficient to up-regulate phosphorylation of a KaiC hexamer to saturated levels (*36*). This is consistent with the higher abundance of KaiC in vivo relative to KaiA (*37*). What is the structural basis of KaiA's function? KaiA binds to the KaiC CII lobe C-terminal tail (*32*). This binding interaction requires concomitant unfolding of an S-shaped loop in the contacted KaiC subunit. We hypothesize that KaiA pulls the S-shaped loop out of the central channel of the KaiC hexameric barrel (Fig. 2). In the KaiC crystal structure, the loop residues (amino acids 485 to 497) are engaged in hydrogen bonding interactions across subunits at the periphery of the channel (Fig. 2B) (*21*). Disrupting the fold of the S-shaped loop of a single subunit might weaken the interface between adjacent CII lobes and promote conformational changes within the CII ring that support phosphorylation at T432 and S431 (*38*). A three-dimensional electron microscopy (EM) structure of the KaiA•KaiC complex reveals that KaiA is connected to the hexameric barrel of KaiC via a flexible linker (*33*). The
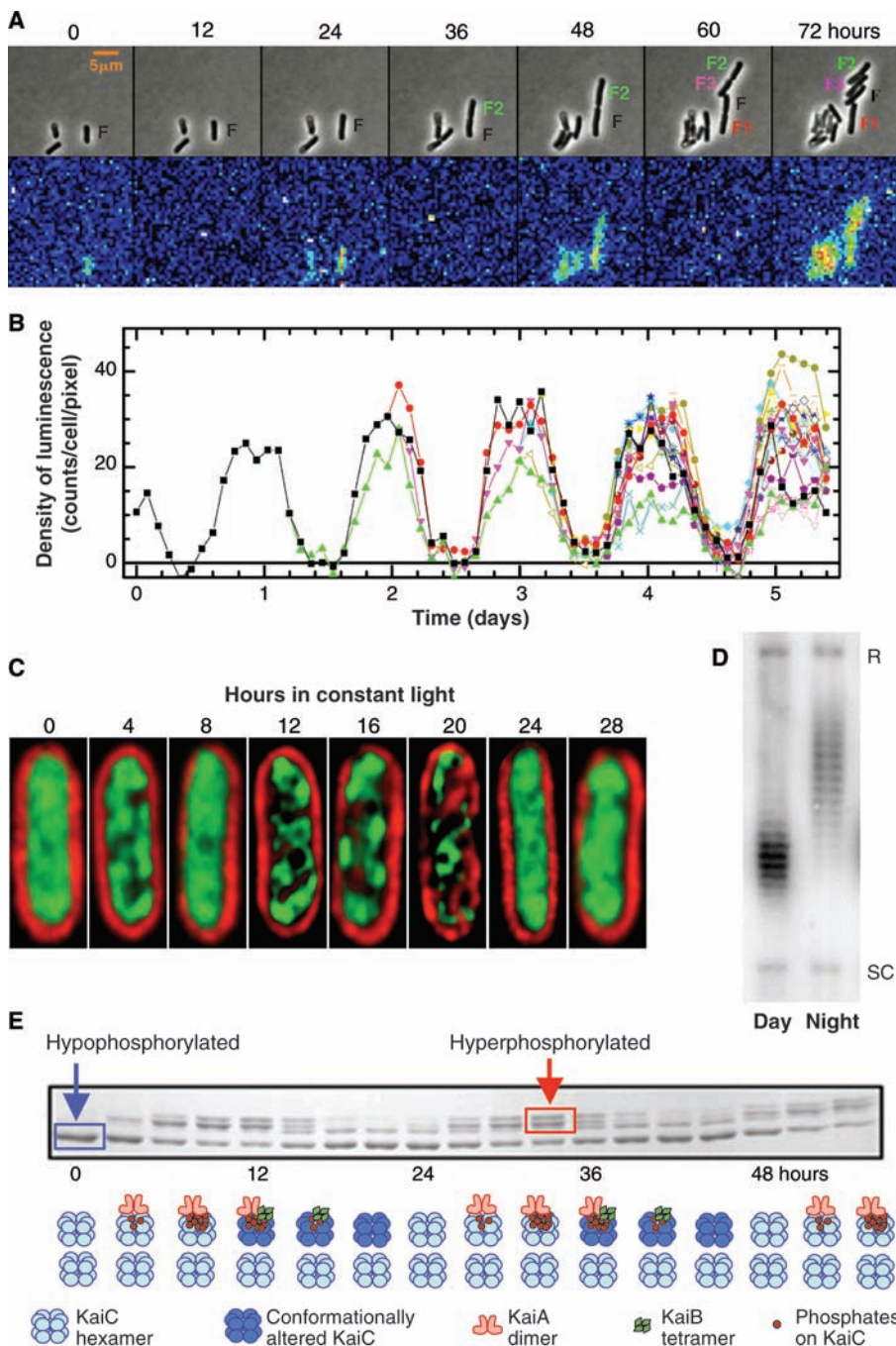


**Fig. 1.** Rhythms in cyanobacteria from cells to molecules. (**A** and **B**) Circadian rhythms of bioluminescence in single cyanobacterial cells. (A) Micrographs of cyanobacterial cells at different times in constant light conditions. (Upper) Brightfield images showing growth and cell division as a function of approximate circadian time; (lower) luminescence emanating from these cells (the luminescence reporter was the *psbAI* promoter driving expression of bacterial luciferase, *luxAB*). (B) Quantification of bioluminescence from a single cell as it divides into multiple cells as a function of time in constant light. Starting at day 1.5, there are two differently colored traces as a result of cell division; the next division occurs at day 2.0, and so on [(A) and (B) are courtesy of I. Mihalcescu, reprinted with permission from (*5*)]. (**C**) Circadian rhythm of chromosomal compaction as visualized by a fluorescent DNA-binding dye (green) (red indicates chlorophyll autofluorescence). The chromosome is more compacted in the subjective night (hours 12 to 20) and less compacted in the subjective day (hours 0 to 8, 24 to 28) [(C) is courtesy of S. Williams, reprinted with permission from (*11*)]. (**D**) Chromosomal topology shows a circadian rhythm as assayed by supercoiling of an endogenous plasmid. Topoisomers of the plasmid are more relaxed (R) in the subjective night and are more supercoiled (SC) in the subjective day (*12*). (**E**) (Upper) KaiC phosphorylation in the oscillating in vitro reaction is shown by SDS-PAGE; upper bands are hyperphosphorylated KaiC, and lower band is hypophosphorylated KaiC. (Lower) The predominant species of complexes of KaiA, KaiB, and KaiC that form during the in vitro oscillation; hypophosphorylated and uncomplexed KaiC hexamers (lower row) are present at all phases, but KaiC in complexes with KaiA and/or KaiB forms rhythmically in concert with changes in KaiC's phosphorylation status (upper line, only the predominant complex is shown). Light blue KaiC hexamers are in the phosphorylating phase before monomer exchange, while dark blue KaiC hexamers are those undergoing dephosphorylation and monomer exchange.

EM structure also suggests that a transient interaction may occur between the apical loop of KaiA and the ATP-binding cleft of KaiC. Thus, the action of KaiA might be to promote conformational flexibility of the KaiCII ring by disrupting the S-shaped loop hydrogen bond network (Fig. 2, C to E) or alternatively, to enhance the residence time of ATP by covering the ATP-binding cleft. Therefore, these interactions of KaiA with KaiC could promote the hyperphosphorylation of KaiC by enhancing its rate of autophosphorylation and/or its ATP residence time.

The binding mode of KaiB to KaiC differs fundamentally from that of KaiA. Unlike KaiA, which is associated with KaiC during the entire phosphorylation cycle, KaiB preferentially binds to the phosphorylated form of the hexamer (28, 30, 31, 35). Structural analyses combining cryo- and negative-stain EM, x-ray crystallography, native polyacrylamide gel electrophoresis (PAGE), and fluorescence methods revealed that KaiB dimers bind to the CII ring (Fig. 3C) (34). Instead of interacting with C-terminal KaiC tails, KaiB dimers form a third layer on top of CII without obscuring the central channel. This arrangement has important consequences for KaiA; although still tethered to the C-terminal CII peptide, KaiA is unable to approach the ATP-binding clefts (Fig. 3D). Thus, the EM structure offers a plausible model for KaiB's antagonism to KaiA. In addition to sequestering KaiA, KaiB may use its conserved, negatively charged C-terminal tail to weaken subunit interactions at the CII side of the KaiC hexamer and to destabilize or displace ATP. Notably, the EM structure of the KaiB•KaiC complex showed no density for the folded S loops, suggesting that they are pulled out of the central channel of the KaiC hexameric barrel when KaiB is bound.

## Why Biological Time Does Not Run Backward

The KaiC crystal structure exhibited double phosphorylation at T432 and S431 in four of the six subunits (21, 24). In the remaining two subunits, only T432 was phosphorylated (Fig. 3A). The T432 side-chain oxygen atoms are closer on average to the ATP $\gamma$-phosphate (7.3 Å) than the S431 side-chain oxygen atoms (8.4 Å); however, neither side chain is in an optimal position for phosphotransfer. This is not surprising because phosphorylated subunits represent the kinase product state and the phosphorylated side chains have presumably moved away from ATP to avoid unfavorable electrostatic interac-

tions. The crystal structure shows a subtle 1 to 2 Å variation in the distances between phosphorylation sites and ATP $\gamma$-phosphates, suggesting that the CII domains have a tendency to flex. Phosphorylation of T432 results in stabilizing interactions between adjacent CII domains (Fig. 3E and fig. S2) (24). The phosphate group is engaged in multiple hydrogen bonds to arginine and serine residues, suggesting that local conformational fluctuations will be more limited after the initial phosphate transfer. If S431 is phosphorylated by a pathway similar to that resulting in T432 phosphorylation, the stabilizing intersubunit interactions formed by P-T432 would have to be broken in order to bring S431 in an optimal position for phospho-transfer from ATP. In a potential alternative mechanism for S431 phosphorylation, S431 could receive a phosphate from P-T432, followed by immediate rephosphorylation of T432. This alternative mechanism would explain the strict order of phosphorylation events (T432 first and S431 second) and is consistent with the structural data.

Once phosphorylated, S431 can engage in additional hydrogen bonding interactions with

amino acids in the same subunit (Fig. 3F and fig. S3). Among the interacting residues is T426, whose mutation to Ala abolishes clock function (24). The configuration observed in the crystal structure for the T432 and S431 phosphate groups of chain f is particularly interesting in that it shows the two phosphate groups in van der Waals contact and stabilized by an interacting arginine (R393; Fig. 3G). This provides structural evidence that T432 and S431 can, in principle, get close enough to each other to allow for a phosphate transfer. Another structural observation supporting the alternative mechanism is that in the two subunits exhibiting phosphorylation only at T432 (chains c and d; Fig. 3A), the side-chain oxygen atom of S431 lies closer to the phosphate of P-T432 (7.0 Å) than to the $\gamma$-phosphate of ATP (8.4 Å). However, the observation that the T432E mutant protein can still be phosphorylated at S431 (28) indicates that phospho-transfer to S431 can occur directly from ATP. Overall, the structural information on the phosphorylation events at the KaiCII subunit interfaces and the inter- and intra-subunit interactions formed by the phosphorylated residues indicates that the number of hydrogen bonds increases as first T432 and subsequently S431 is phosphorylated. This progressive increase in molecular interaction would make the reverse reactions unfavorable, causing a built-in ratcheting mechanism that drives the KaiC oscillator unidirectionally.

We envision that a conformational change is then required to drive KaiC forward to the phosphatase state and achieve dephosphorylation first of T432 and then of S431 in all six subunits. Sequential dephosphorylation in this order has been observed in biochemical assays (28, 35). Interaction of KaiB with KaiC facilitates the formation of the phosphatase state. Unlike KaiA, which has similar affinities for various forms of KaiC (30), KaiB binds preferentially to the hyperphosphorylated form of KaiC (specifically, P-S431) (28, 35). KaiC can thus be either a kinase or a phosphatase; at present, only the kinase state has been captured in a high-resolution crystal structure. Some of the outstanding questions for further research on the biochemistry of these key reactions include understanding the mechanism of monomer exchange, the configuration of KaiC in the unphosphorylated state, and the means by which KaiC can dephosphorylate.

## How Does This in Vitro Clockwork Tick?

The unexpected demonstration that KaiC's phosphorylation status continued to cycle when the three Kai
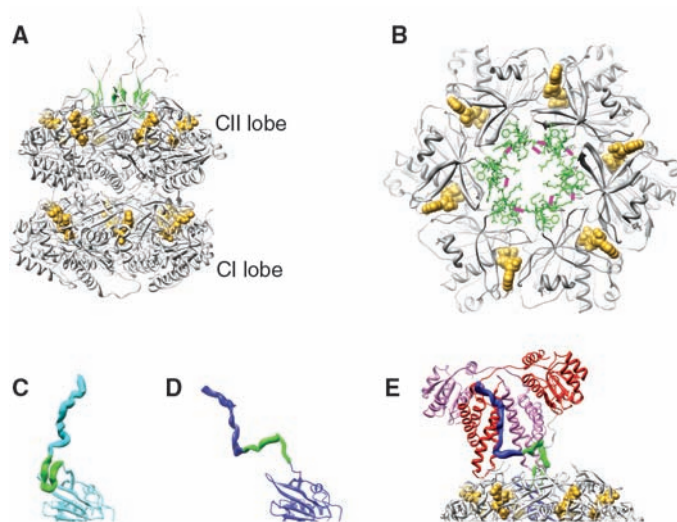


**Fig. 2.** KaiA-KaiC interaction. (**A**) The crystal structure of the KaiC hexamer shows a double doughnut shape formed by two lobes per subunit [Protein Data Bank (PDB) ID 2GBL]. The S-shaped loops (amino acids 485 to 497) (green) dip into the central channel of the hexameric barrel. The flexible C-terminal residues (amino acids 498 to 519) extend from the CII end of the hexamer. Some of the C-terminal tails are shorter than others because this region is partly disordered and only two chains have been completely traced out to the C-terminal S519 residue. ATP (gold) is bound between subunits in both the lower CI ring and the upper CII ring. (**B**) The six S-shaped loops (green stick representation) interact via a hydrogen bond network. Hydrogen bonds are shown in magenta and the view is perpendicular to (A) as seen from the CII side. (**C**) The CII end of one KaiC monomer as in the crystal structure with the S-shaped loop in green. (**D**) The CII end of one KaiC monomer as proposed to interact with KaiA, with the S-shaped loop pulled out (33). In (C) and (D), the S-shaped loop and C-terminal tail are shown as a wide ribbon. (**E**) Model of the KaiA-KaiC interaction based on combined structural information from x-ray crystallography, nuclear magnetic resonance, and three-dimensional EM (33). One S-shaped loop (green) is shown pulled out of the KaiC hexameric barrel. For clarity, the S-shaped loop and C-terminal residues are shown for only one of the six KaiC subunits. The KaiA dimer is shown in red and purple.

proteins are combined in a test tube and ATP was added to provide energy (Fig. 1E) (*22*) shows that circadian oscillations are not absolutely dependent upon transcriptional and/or translational feedback (*22, 27, 39, 40*). The in vitro rhythm, KaiC's dephosphorylation rate, and KaiC's ATP hydrolytic activity are all temperature compensated (*22, 29, 40*); that is, a temperature compensation mechanism is intrinsic to the characteristics of the three Kai proteins and the nature of their interactions. How this is accomplished is an important unresolved question for the cyanobacterial system and for circadian clocks in general (*22, 29, 40*).

The availability of the in vitro system for analyzing the molecular nature of a circadian clockwork allows biophysical, biochemical, and structural analyses that were previously impossible. EM, chromatography, and native gel electrophoresis techniques have been applied to quantify the time-dependent formation of complexes among the Kai proteins (*30, 31*). KaiC exists in all possible combinations with KaiA and KaiB throughout the in vitro oscillation: free KaiC hexamers, KaiA•KaiC complexes, KaiB•KaiC complexes, and KaiA•KaiB•KaiC complexes (Fig. 1E). The proportions of these complexes vary in a phase-dependent manner: Free KaiC hexamers predominate at all phases; ~10% of KaiC hexamers appear as KaiA•KaiC complexes at all phases; and KaiB•KaiC and KaiA•KaiB•KaiC complexes are clearly rhythmic, becoming most common in the KaiC dephosphorylation phase (Fig. 1E) (*30, 31*). Therefore, during the in vitro oscillation, KaiC is undergoing rhythmic changes in conformation, phosphorylation status, and interactions with KaiA and KaiB. As structural studies have indicated, changes in the KaiC phosphorylation/dephosphorylation status correlate with conformational changes in KaiC. The central core of the oscillator is probably the rhythm of changes in KaiC conformation that modulate interactions with KaiA and KaiB and influence the activity of transduction factors such as SasA and RpaA (*13, 30, 31*), whereas the role of the KaiC phosphorylation/dephosphorylation is to facilitate the changes of KaiC conformation that mediate these interactions.

Maintenance of a high-amplitude oscillation in the face of noise is a crucial characteristic of any circadian oscillator (*5*). In the case of the in vitro oscillator, KaiC monomers exchange among
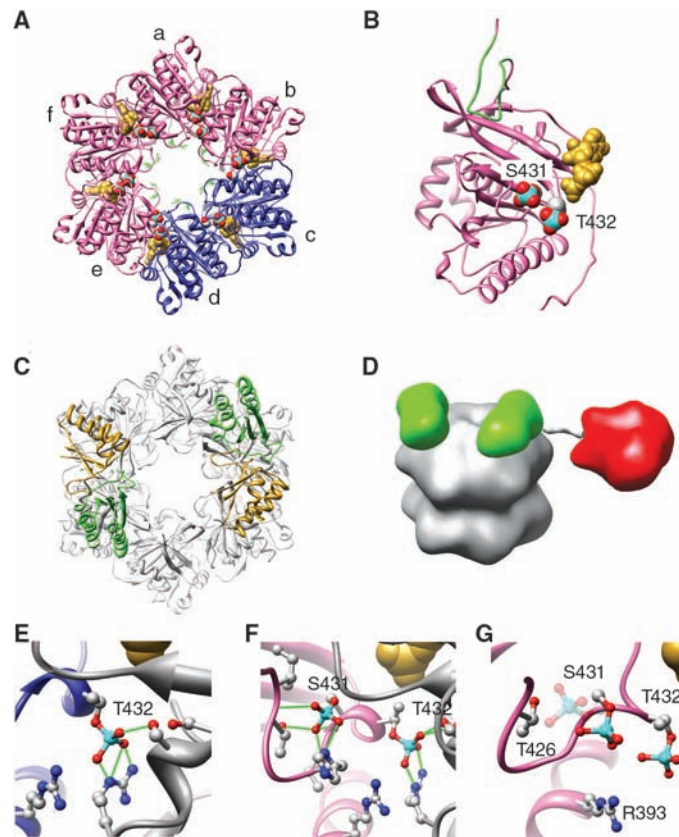


**Fig. 3.** Structural stabilization mediated by phosphorylation and KaiB-KaiC interaction. (**A**) Ring of CII lobes from the KaiC crystal structure. Four subunits, chains a, b, e, and f (pink), are doubly phosphorylated at S431 and T432. Two subunits, chains c and d (blue), are singly phosphorylated at T432. The side chains of S431 and T432 are shown in space-filling representation and are colored by element with phosphorus atoms in cyan and oxygen atoms in red. ATP (gold) is bound between the CII lobes. (**B**) CII lobe of a doubly phosphorylated KaiC monomer (chain a) with the S-shaped loop in green. The view is perpendicular to (A). (**C**) Model of the KaiB•KaiC interaction based on combined structural information from x-ray crystallography and three-dimensional EM (*34*) with KaiB dimers in green and gold. (**D**) Model of the KaiA•KaiB•KaiC interaction with KaiA (red) and KaiB (green) dimers in orientations resembling those in the class IV KaiABC particle images from negative-stain EM [see figure 1D in (*31*)]. (**E**) Hydrogen bonds (green) formed by the phosphate group of T432 in chain c (blue). (**F**) Hydrogen bonds formed by the phosphate groups of S431 and T432 in chain b (pink). In (E) and (F), the neighboring chain is shown in gray. See figs. S2 and S3 for the hydrogen bonds formed by the additional phosphate groups in chains a to f. (**G**) In chain f, the phosphate group of S431 is leaning toward T432, rather than toward T426 as in chains a, b, and e. The position of the S431 phosphate group in chain e is shown in a faint representation. The phosphate groups of both S431 and T432 in chain f are stabilized by electrostatic interactions with R393.

the hexamers, a process that synchronizes the phosphorylation status of the individual hexamers in the population of hexamers (Fig. 4) (*23, 30, 31*). Consequently, although cyanobacterial cells in populations are autonomous oscillators that do not communicate phase information intercellularly (*5*), communication among KaiC hexamers via monomer exchange maintains a high-amplitude rhythm inside the cell (*23, 31*). Therefore, the posttranslational cyanobacterial clockwork is composed of biochemical reactions such as phosphorylation, ATP hydrolysis, monomer exchange, and conformational changes among thousands of molecules per cell (~10,000 KaiC monomers per cell) (*37*), permitting robust oscillations of high precision and synchrony.

### From Test Tube to Cell; Embedding the KaiABC Oscillator Within a Transcription and Translation Feedback Loop

What is the role of the posttranslational KaiABC oscillator in the overall cellular program (Fig. 4)? There is a rhythm of KaiC phosphorylation in vivo that continues in the absence of transcription or translation, but there are also rhythms of KaiB and KaiC abundance in metabolically active cells that have been interpreted in terms of a transcription and translation feedback loop (TTFL) (*40, 41*). Perhaps the rhythms of KaiC phosphorylation and abundance are complementary processes that can oscillate independently or can interact to generate a more robust overall program (*42*). Early evidence for a core TTFL oscillator in cyanobacteria was partly based on experiments in which KaiC abundance was experimentally manipulated in vivo; KaiC expression from an inducible promoter reset the cellular clock in a phase-dependent manner (*15, 41*). Although the most direct impact of KaiC expression is upon abundance, such expression could also perturb the phosphorylation oscillator; flooding KaiC pools with newly synthesized and therefore unphosphorylated KaiC would be expected to alter the phosphorylation ratio of the KaiC pool. If the new synthesis of KaiC occurs at a phase when hexamers are predominantly hypophosphorylated, the oscillation of KaiC phosphorylation would be reinforced (enhanced amplitude). By contrast, new synthesis of unphosphorylated KaiC when hexamers are predominantly hyperphosphorylated would lead to an overall decrease in the KaiC phosphorylation status, thereby altering the phase of the KaiABC oscillator (phase shift) and/or reducing its amplitude. Therefore, the posttranslational oscillator (PTO) may regulate the timing of transcription and translation to occur in an optimal phase to enhance robustness of the larger oscillating system (Fig. 4). In this scenario, the PTO is embedded in a TTFL; the PTO may most directly determine the dynamics of the circadian system, but the TTFL provides a secondary feedback loop that aids robustness.
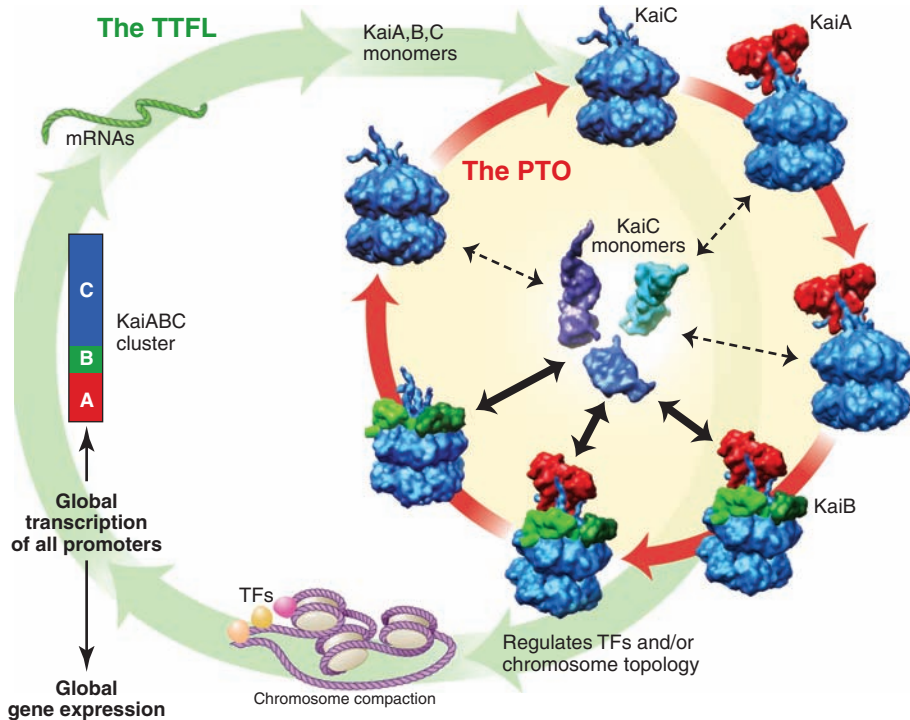
**Fig. 4.** A self-sustained posttranslational oscillator (PTO) embedded within a transcription and translation feedback loop (TTFL). The posttranslational KaiABC oscillator (cycle connected by red arrows) is determined by phosphorylation of KaiC (blue hexamers) as regulated by interactions with KaiA (red dimers) and KaiB (green tetramers). Robustness is maintained by synchronization of KaiC hexameric status via exchange of KaiC monomers (23, 30, 31). Monomer exchange is depicted in the center of the PTO by KaiC monomers exchanging among KaiC hexamers; phase-dependent changes in the rate of monomer exchange are indicated by the thickness of the double-headed black arrows. New synthesis of KaiC feeds into the KaiABC oscillator as nonphosphorylated hexamers or as monomers that exchange into preexisting hexamers. The PTO brings KaiC to a state that regulates chromosome topology and/or transcriptional factors ("TFs") to control global transcription of all promoters (including those driving expression of the essential clock genes *kaiA*, *kaiB*, and *kaiC*).

What are the potential benefits of a biochemical (PTO) oscillator embedded within a genetic (TTFL) oscillator? A core oscillator that is composed of biochemical reactions among thousands of molecules per cell should be more robust in the face of metabolic noise than one founded on transcriptional activity. This is particularly true for cells that must maintain precise timekeeping during cell division, when the ratio of DNA to transcriptional factors can change during replication and where DNA can become less accessible when chromosomes condense in preparation for division. The advantage provided by a biochemical oscillator such as KaiABC is that this posttranslational system would be less susceptible to the influences of cell division (5–8) or major changes in metabolic rate (40, 41) than one based on transcriptional and translational rates. Although eukaryotic circadian genes are not homologous to *kaiABC* sequences, the proteins they encode also undergo circadian rhythms of abundance and phosphorylation (1, 43, 44). The benefit of a clockwork that is imperturbable even when buffeted by the massive intracellular changes of cell division could have provided an evolutionary driving force for convergent circadian clock mechanisms among diverse organisms.

We now recognize KaiABC as a dynamically oscillating nanomachine that has evolved to precess unidirectionally and robustly. The challenges ahead are to delve deeper into the molecular nature of its temperature compensation, to examine the place of the PTO in the larger cellular program, and to discover if the clocks in our own cells have attributes that are similar to those of bacteria.

### References and Notes

1. J. C. Dunlap, J. J. Loros, P. J. DeCoursey, Eds., *Chronobiology: Biological Timekeeping* (Sinauer, Sunderland, MA, 2004).
2. S. R. Mackey, S. S. Golden, *Trends Microbiol.* **15**, 381 (2007).
3. C. H. Johnson, in *Methods in Enzymology*, M. W. Young, Ed. (Academic Press, New York, 2005), vol. 393, pp. 818–837.
4. T. Kondo et al., *Proc. Natl. Acad. Sci. U.S.A.* **90**, 5672 (1993).
5. I. Mihalcescu, W. Hsing, S. Leibler, *Nature* **430**, 81 (2004).
6. T. Mori, B. Binder, C. H. Johnson, *Proc. Natl. Acad. Sci. U.S.A.* **93**, 10183 (1996).
7. T. Kondo et al., *Science* **275**, 224 (1997).
8. T. Mori, C. H. Johnson, *J. Bacteriol.* **183**, 2439 (2001).
9. Y. Liu et al., *Genes Dev.* **9**, 1469 (1995).
10. M. Katayama, N. F. Tsinoremas, T. Kondo, S. S. Golden, *J. Bacteriol.* **181**, 3516 (1999).
11. R. M. Smith, S. B. Williams, *Proc. Natl. Acad. Sci. U.S.A.* **103**, 8564 (2006).
12. M. A. Woelfle, Y. Xu, X. Qin, C. H. Johnson, *Proc. Natl. Acad. Sci. U.S.A.* **104**, 18819 (2007).
13. N. Takai et al., *Proc. Natl. Acad. Sci. U.S.A.* **103**, 12109 (2006).
14. J. R. Chabot, J. M. Pedraza, P. Luitel, A. van Oudenaarden, *Nature* **450**, 1249 (2007).
15. M. Ishiura et al., *Science* **281**, 1519 (1998).
16. M. Egli, R. Pattanayek, S. Pattanayek, in *Models, Mysteries and Magic of Molecules*, J. C. A. Boeyens, J. F. Ogilvie, Eds. (Springer, Dordrecht, Netherlands, 2007), pp. 283–299.
17. S. Ye, I. Vakonakis, T. R. Ioerger, A. C. LiWang, J. C. Sacchettini, *J. Biol. Chem.* **279**, 20511 (2004).
18. K. Hitomi, T. Oyama, S. Han, A. S. Arvai, E. D. Getzoff, *J. Biol. Chem.* **280**, 19127 (2005).
19. R. G. Garces, N. Wu, W. Gillon, E. F. Pai, *EMBO J.* **23**, 1688 (2004).
20. I. Vakonakis et al., *Proc. Natl. Acad. Sci. U.S.A.* **101**, 1479 (2004).
21. R. Pattanayek et al., *Mol. Cell* **15**, 375 (2004).
22. M. Nakajima et al., *Science* **308**, 414 (2005).
23. H. Ito et al., *Nat. Struct. Mol. Biol.* **14**, 1084 (2007).
24. Y. Xu et al., *Proc. Natl. Acad. Sci. U.S.A.* **101**, 13933 (2004).
25. T. Nishiwaki et al., *Proc. Natl. Acad. Sci. U.S.A.* **101**, 13927 (2004).
26. H. Iwasaki, T. Nishiwaki, Y. Kitayama, M. Nakajima, T. Kondo, *Proc. Natl. Acad. Sci. U.S.A.* **99**, 15788 (2002).
27. Y. Xu, T. Mori, C. H. Johnson, *EMBO J.* **22**, 2117 (2003).
28. T. Nishiwaki et al., *EMBO J.* **26**, 4029 (2007).
29. K. Terauchi et al., *Proc. Natl. Acad. Sci. U.S.A.* **104**, 16377 (2007).
30. K. Kageyama et al., *Mol. Cell* **23**, 161 (2006).
31. T. Mori et al., *PLoS Biol.* **5**, e93 (2007).
32. I. Vakonakis, A. C. LiWang, *Proc. Natl. Acad. Sci. U.S.A.* **101**, 10925 (2004).
33. R. Pattanayek et al., *EMBO J.* **25**, 2017 (2006).
34. R. Pattanayek et al., *EMBO J.* **27**, 1767 (2008).
35. M. J. Rust, J. S. Markson, W. S. Lane, D. S. Fisher, E. K. O'Shea, *Science* **318**, 809 (2007).
36. F. Hayashi et al., *Biochem. Biophys. Res. Commun.* **316**, 195 (2004).
37. Y. Kitayama, H. Iwasaki, T. Nishiwaki, T. Kondo, *EMBO J.* **22**, 2127 (2003).
38. Y. I. Kim, G. Dong, C. W. Carruthers, S. S. Golden, A. LiWang, *Proc. Natl. Acad. Sci. U.S.A.* **105**, 12825 (2008).
39. Y. Nakahira et al., *Proc. Natl. Acad. Sci. U.S.A.* **101**, 881 (2004).
40. J. Tomita, M. Nakajima, T. Kondo, H. Iwasaki, *Science* **307**, 251 (2005).
41. Y. Xu, T. Mori, C. H. Johnson, *EMBO J.* **19**, 3349 (2000).
42. Y. Kitayama, T. Nishiwaki, K. Terauchi, T. Kondo, *Genes Dev.* **22**, 1513 (2008).
43. G. Huang et al., *Genes Dev.* **21**, 3283 (2007).
44. M. Gallego, D. M. Virshup, *Nat. Rev. Mol. Cell Biol.* **8**, 139 (2007).
45. We thank our colleagues and coauthors at Vanderbilt University, especially M. Byrne, T. Mori, X. Qin, R. Pattanayek, S. Pattanayek, D. Williams, M. Woelfle, and Y. Xu. We also thank T. Kondo, S. Golden, M. Ishiura, and their laboratory members whose seminal contributions continue to make the study of cyanobacterial clocks fascinating. Supported by funds from the NIH, specifically the National Institute of General Medical Sciences (grant GM067152 to C.H.J. and grant GM073845 to M.E.). Additional support from the NIH (grant F32 GM71276 to D. R. Williams in the Stewart laboratory) is gratefully acknowledged.

# Supporting Online Material for

## Structural Insights into a Circadian Oscillator

Carl Hirschie Johnson,[*] Martin Egli, Phoebe L. Stewart

*To whom correspondence should be addressed. E-mail: carl.h.johnson@vanderbilt.edu
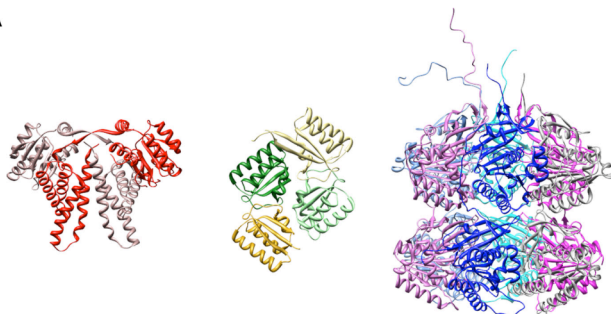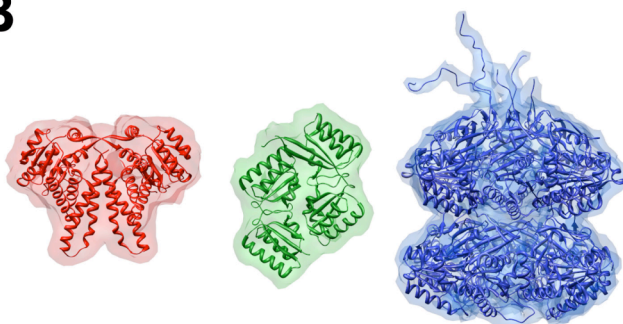
**This PDF file includes:**

Figs. S1 to S3
References

# SUPPORTING ONLINE MATERIAL FOR:

## Structural Insights into a Circadian Oscillator

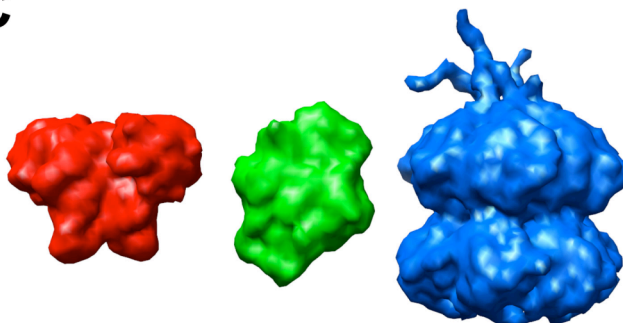Carl Hirschie Johnson, Martin Egli, Phoebe L. Stewart

**A**

**B**

**C**



**Supplemental Figure S1. High resolution crystal structures of the cyanobacterial clock proteins KaiA, KaiB, and KaiC.** (A) Crystal structures of the *S. elongatus* KaiA dimer (PDB-ID 1R8J, ref. *S1*); the *Synechocystis* KaiB tetramer (PDB-ID 1WWJ, ref. *S2*; the crystal structures for KaiA and KaiB from *Anabaena* have also been published in ref. *S3*); and the *S. elongatus* KaiC hexamer (PDB-ID 2GBL; refs. *S4 & S5*). Each subunit is colored differently. (B) The crystal structures of KaiA, KaiB and KaiC together with transparent density envelopes representing the structures filtered to 10 Å resolution. (C) Density representations of KaiA, KaiB and KaiC at 10 Å resolution to reveal the overall shapes of the molecules. The molecular graphics images were produced with the UCSF Chimera package (*S6*).
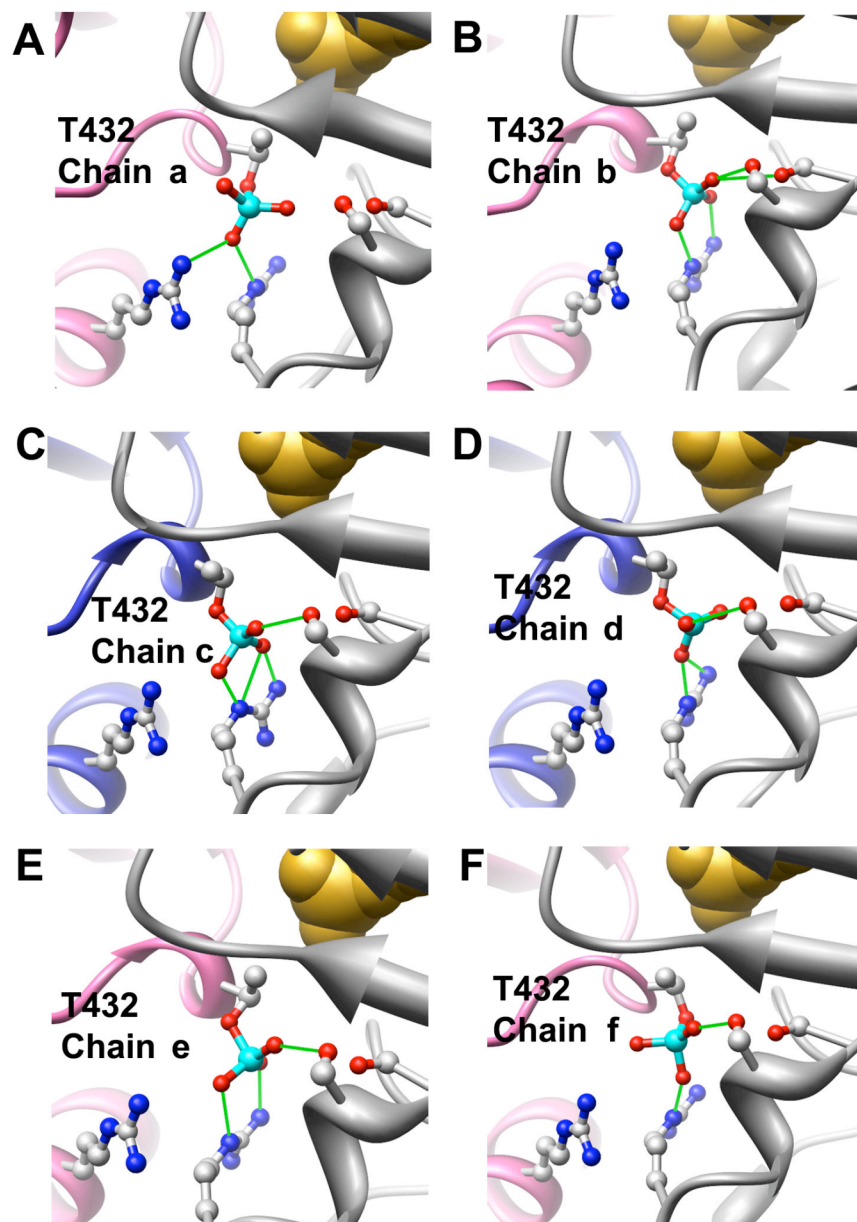
**Supplemental Figure S2. Hydrogen bonds formed by the phosphate group of Thr-432 (T432).** In the KaiC crystal structure all six chains of the KaiC hexamer are phosphorylated at T432. Views of the regions surrounding T432 in chains a,b,c,d,e and f in panels (A) through (F). Chains c and d (blue ribbon) are singly phosphorylated at T432. Chains a, b, e and f (pink ribbons) are doubly phosphorylated at S431 (see Fig. S3) and T432. In each case the neighboring chain in the hexamer is shown in gray. Note that almost all of the hydrogen bonds formed by the T432 phosphate groups are between two chains of the KaiC hexamer. Sidechains are depicted for T432 as well as for the nearby residues (S379, S381, R385, R393) that form a hydrogen bonding pocket for T432. Hydrogen bonds are shown in green, ATP molecules are in a space filling representation (gold), and sidechain atoms are colored by element with phosphorus in cyan.
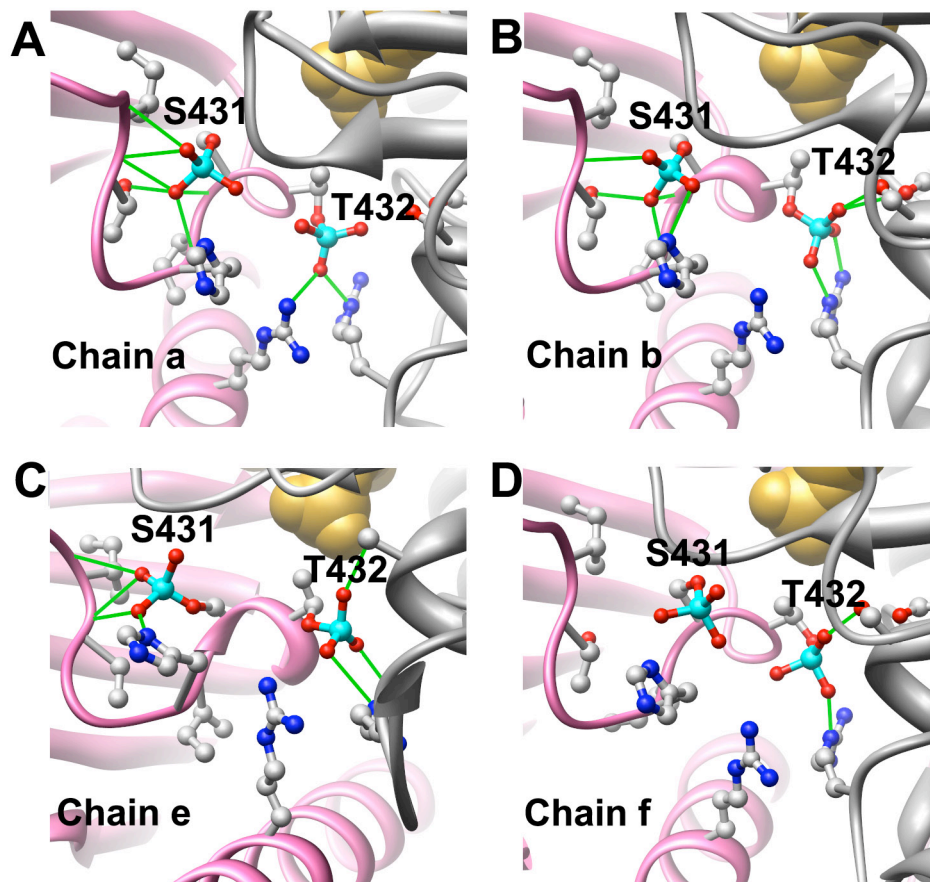
**Supplemental Figure S3. Hydrogen bonds formed by the phosphate group of Ser-431 (S431).** In the KaiC crystal structure four of the six chains of the KaiC hexamer are phosphorylated at S431. Views of the regions surrounding S431 in chains a,b,e and f are depicted in panels (A) through (D). In each case the neighboring chain in the hexamer is shown in gray. Sidechains are depicted for S431 and T432 as well as for the nearby residues (I425, T426, H429, I430) that form a hydrogen bonding pocket for S431 and for T432 (S379, S381, R385, R393). Note that many of the hydrogen bonds formed by the S431 phosphate groups are to backbone nitrogen atoms. Hydrogen bonds are shown in green, ATP molecules are in a space filling representation (gold), and sidechain atoms are colored by element with phosphorus in cyan.

# References for Supplement

S1. Ye S, Vakonakis I, Ioerger TR, LiWang AC, Sacchettini JC (2004) Crystal structure of circadian clock protein KaiA from *Synechococcus elongatus*. J Biol Chem 279: 20511-20518.

S2. Hitomi K, Oyama T, Han S, Arvai AS, Getzoff ED (2005) Tetrameric architecture of the circadian clock protein KaiB: a novel interface for intermolecular interactions and its impact on the circadian rhythm. J Biol Chem 280: 18643-18650.

S3. Garces RG, Wu N, Gillon W, Pai EF (2004) *Anabaena* circadian clock proteins KaiA and KaiB reveal a potential common binding site to their partner KaiC. EMBO J 23: 1688-98.

S4. Pattanayek R, Wang J, Mori T, Xu Y, Johnson CH, and Egli M (2004) Visualizing a circadian clock protein: crystal structure of KaiC and functional insights. Mole Cell 15: 375–388.

S5. Pattanayek R, Williams DR, Pattanayek S, Xu Y, Mori T, Johnson CH, Stewart PL, Egli M (2006) Analysis of KaiA-KaiC protein interactions in the cyanobacterial circadian clock using hybrid structural methods. EMBO J 25:2017-2038.

S6. Pettersen EF, Goddard TD, Huang CC, Couch GS, Greenblatt DM, Meng EC, Ferrin TE (2004) UCSF Chimera - a visualization system for exploratory research and analysis. J Comput Chem 25: 1605-1612.